JOURNAL OF Applied Polymer SCIENCE

Influence of Chemical Treatment on the Properties of Banana Stem Fiber and Banana Stem Fiber/Coir Hybrid Fiber Reinforced Maleic Anhydride Grafted Polypropylene/Low-Density Polyethylene Composites

G. M. Arifuzzaman Khan,[1] M. S. Alam Shams,[1] Md. R. Kabir,[1] M. A. Gafur,[2] M. Terano,[3] M. S. Alam[1]

[1]Polymer Research Laboratory, Department of Applied Chemistry and Chemical Technology, Islamic University, Kushtia, Bangladesh

[2]Pilot Plant (PP) and Product Development Centre (PDC), Bangladesh Council of Scientific and Industrial Research (BCSIR) Laboratory, Dhaka, Bangladesh

[3]School of Materials Science, Japan Advanced Institute of Science and Technology, Japan

Correspondence to: M. S. Alam (E-mail: dr.alamiu@yahoo.com)

ABSTRACT: Banana stem fiber (BSF) reinforced low-density polyethylene (PE) composites were prepared with a hot-press molding machine in the presence of maleic anhydride grafted polypropylene (MAPP). To achieve better mechanical properties, the fiber was chemically modified by bleaching, alkalization, and acetylation. The ultimate tensile strength (UTS) of the untreated and treated BSF composites were found to increase with increasing fiber loading up to 20%, whereas the maximum Charpy impact strength (IS) and flexural strength (FS) values were seen at 10% fiber loading; these values decreased thereafter. The Young's modulus (YM) values of the BSF composites increased sharply with fiber loading. All of the treated fibers exhibited better mechanical properties than the untreated ones. The acetylated fiber showed higher UTS (44 MPa), FS (50 MPa), and IS (12.5 j/m^2) values than the other treated and untreated fibers. The improvements in the mechanical properties of the treated composites were further supported by scanning electron microscopy images of the fracture surfaces. The thermal stabilities of the composites were studied by means of thermogravimetry, differential thermogravimetry, and differential thermal analysis measurements. Hybrid composites composed of BSF (10 wt %), coir fiber (5 wt %), and a MAPP/low-density PE matrix were prepared. Significant improvements in UTS, YM, FS, and IS were seen in the hybrid composites containing surface-modified BSF. The effects of BSF composition on the composite properties were also studied. © 2012 Wiley Periodicals, Inc. J. Appl. Polym. Sci. 000: 000–000, 2012

KEYWORDS: biofibers; composites; morphology; mechanical properties

Received 31 July 2011; accepted 11 June 2012; published online
DOI: 10.1002/app.38197

INTRODUCTION

Nowadays, natural fibers play important roles in the aircraft, automobile, electronics, and medical industries as alternatives to timber, concrete, steel, glass fiber, and so on. The use of natural-fiber-reinforced plastic composites has recently gained importance and popularity because of their light weight, high tensile strength, high stiffness, corrosion resistance, lower impact on the environment, and so on. Natural fibers have a high tensile modulus (20–130 GPa) that is nearer to that of glass fiber (70 GPa).[1] Their composites are superior to any other building materials as they are ecofriendly to a large extent; this is important in today's environment. Extensive studies of the preparation and properties of thermoplastic/thermosetting plastics composites filled with jute, bamboo, sisal, coir, hemp, flax, pineapple leaf fiber, and banana stem fiber (BSF) have been carried out.[2–6] Despite their advantages, their use has been restricted because of their inherent high moisture absorption capacities, thermal instability during processing, the presence of lignin and hemicellulose,[7] and poor adhesion to commercial synthetic polymers.

The degree of chemical bonding between the cellulose fibers, and the polymer matrix controls the amount of stress transferred via the interface.[8,9] However, it is very rare to build good interfacial bonding between the chemically different matrix and fiber. A compatibilizer would be required during the fabrication of the composites for better interfacial bonding. Maleated compounds are widely used for this purpose. In most cases, scientists have used matching maleated compounds with the polymer matrix, such as maleic anhydride grafted polypropylene (MAPP) and polypropylene (PP)

Table I. Physical Properties of the BSF and Coir Fiber

Fiber	Diameter (μm)	Density (kg/m^3)	Cell ratio (length/diameter)	Cellulose (%)	Hemicellulose (%)	Lignin (%)
Untreated BSF	180 ± 24	1302	142	63–64	19	5
Bleached BSF	160 ± 21	1401	140	85	15	0
Alkali-treated BSF	154 ± 20	1400	138	90	4	6
Acetylated BSF	165 ± 18	1390	140	—	—	—
Coir fiber	305 ± 42	1130	36	45–50	20–25	30

or Maleated polyethylene (MAPE) and low-density polyethylene (LDPE). Dikobe and Luyt[10] showed that MAPP/linear low-density polyethylene (LLDPE)/wood powder also showed better properties due to strong interfacial interactions between the MAPP, LLDPE, and wood powder.

Although fiber cellulose has very reactive alcoholic hydroxyl groups, these are blocked by encrusting materials, such as lignin, hemicelluloses, and pectin. Various surface modification techniques, such as mercerization, oxidation bleaching, cyanoethylation, acetylation, coupling agent treatment, and γ-ray irradiation, have been used to improve fiber/matrix interfacial bonding during composite fabrication.[11–15] Mercerization (alkali treatment) is the most common chemical process; it removes noncellulose components and a part of the amorphous cellulose.[16,17] Alkaline treatments also have a lasting effect on the mechanical behavior of the fiber, especially the fiber strength and stiffness. The acetylation of cellulose fiber is also a well-known esterification method, which causes the plasticization of cellulose fibers. Hydroxyl groups of cellulose fiber with acetyl groups can modify the properties of polymers so that they become hydrophobic; this can stabilize the fiber against moisture and improve the dimension stability and environmental degradation.[18] Acetic anhydride in the presence of fatty acids is very commonly used to prepare reinforcing elements for composites with common thermoplastic matrices such as polyethylene. Bleaching technology is widely used in textiles to remove coloring materials. Bleaching may also increase the surface roughness of the fiber and result in improved mechanical interlocking with the polymer matrix.[19]

Hybrid filler composite materials have caught the attention of researchers in the last few years. These introduce additional degrees of compositional freedom and provide yet another dimension to the potential versatility of fiber-reinforced composites. Jacob et al.[20,21] studied the tensile properties and curing characteristics of sisal/oil palm hybrid fiber-reinforced natural rubber composites. Paiva Junior et al.[22] showed that ramie fibers have a high potentiality and that cotton makes a weak contribution as a reinforcement to hybrid ramie/cotton fabrics/polyester composites. Therefore, the composition and properties of natural fibers have great potential to improve the composite properties.

BSF, which is now present in huge amounts in agricultural waste (annual world production = 100,296 tons), contains α-cellulose (63–64 wt %), hemicelluloses (17 wt %), and lignin (5.0 wt %).[23] Because of its low production cost ($0.03 US/kg), high crystallinity[24] (45%), high tensile strength (70–200 MPa), and high decomposition temperature (353°C), a number of scientists have used it to make composites with polyolefin, polyester, and so on.[25,26] In this study, short untreated BSF, bleached BSF, alkalized BSF, acetylated BSF, and BSF/coir hybrid fibers were used to prepare composites with an LDPE matrix. The effects of different proportions of fiber constituents on the composite properties were also considered.

EXPERIMENTAL

Materials

Discarded BSF and coir fiber were collected from an agricultural farm at Kushtia, Bangladesh. The fibers were extracted by water retting and washed with sodium carbonate and detergents. The properties of the fibers are listed in Table I. Acetic acid (100 wt %), acetic anhydride (99.5 wt %), sodium hydroxide (>99.5 wt %), LDPE (tensile strength = 0.2–0.4 N/mm^2, mp = 110°C, glass-transition temperature = −125°C, density 0.91–0.94 g/cm^3) were supplied by Merck (Germany). MAPP was purchased from Sigma-Aldrich (USA), and its maleic anhydride content about 8 wt %. The number-average molecular weight and weight-average molecular weight/number-average molecular weight were 3.9 × 10^3 and 2.3, respectively.

Fiber Treatment

The fiber was cut into pieces approximately 15 cm long. Then, the lignin from fibers were removed by a bleaching operation with a 7 mg/L $NaClO_2$ solution at pH 4 (buffered by CH_3COOH and CH_3COONa) for 90 min at 353–363 K. The fiber-to-liquor ratio was maintained at 1 : 50. After the reaction was complete, the fiber was washed several times with cold distilled water. Then, the bleached fiber was treated with a 0.2% sodium metabisulfite ($Na_2S_2O_5$) solution for 15 min and finally washed with distilled water.

The untreated BSF was soaked in a 5% NaOH solution in a water bath where the temperature was maintained at 303 K for 10 h and the fiber-to-liquor ratio was 1 : 50. The treated fiber was rinsed several times and left to dry at room temperature.

An amount of 10 g of bleached BSF was soaked in glacial acetic acid for 1 h at room temperature. The acid was decanted, and soaking was continued in acetic anhydride (50 mL) containing two drops of concentrated sulfuric acid for 10 min at a fiber-to-liquor ratio of 1 : 50. The fiber was separated with a Buchner funnel, washed with water, and dried in oven at 323 K for 24 h.

The main constituents of BSF and coir fiber were isolated according to a TAPPI standard.[27]

Table II. Changes in the Composite Density with Fiber Loading

MAPP/LDPE/untreated BSF (wt %)	Density (g/cm^3)
5/95/0	0.90
5/85/10	0.82
5/75/20	0.75
5/65/30	0.68

Fiber Testing

The infrared (IR) spectra of the untreated and treated BSF were recorded with a Shimadzu IR-470 spectrophotometer (Shimadzu, Kyoto, Japan) with the KBr pellet technique. A mixture of 5 mg of dried fibers and 200 mg of KBr were pressed into a disk for IR measurement.

Composite Preparation

Dried BSF (at 5, 10, 20, and 30 wt %) and 5 wt % MAPP were initially mixed thoroughly with LDPE with a single-screw extruder at 433 K. The composites were made with a stainless steel mold measuring 150 × 150 × 40 mm^3 (Length × Width × Depth). The releasing agent, PAT 607/PCM, was sprayed onto a laboratory tissue and smeared evenly onto the surface of the mold. The mixture was cut into small pieces and spread uniformly on the surfaces of the molds. Polymer composite sheets were prepared by the hot pressing of the mold at 433 ± 5 K for 30 min. The pressure applied ranged from 50 kN, depending on the loading of the reinforcing material. Cooling was done with tap water through the outer area of the heating plates of the Paul–Otto–Weber press machine (China). The specimen were demolded and postcured at 50°C for 12 h. The composite sheets were cut for mechanical testing according to an ASTM standard.

Composite Testing

The ultimate tensile strength (UTS) and Young's modulus (YM) values of the BSF composites were measured with an Instron 3366 on the basis of ASTM D 3822-01 and ASTM D 1043-09, respectivly. The gage length and crosshead speed were fixed at 20 mm and 5 mm/min, respectively. Three-point flexural tests of the composites were carried out with the Instron 3366 according to the standard method used for flexural properties (ASTM D 790-98). The speed for the flexural test was set at 5 mm/min. Notched Charpy impact tests (according to ASTM D 6110-97) were carried out with a Universal Impact tester-(cometech) Taiwan, Extruder- Dynisco, Heilbronn, Germany. All of the results were taken as the average value of 10 samples.

Scanning electron microscopy (SEM) was used to observe the microstructures and surface morphologies of the untreated BSF, treated BSF, and their composites. The instrument (Philips XL-30 SEM Instrument- Germany) was operated with an excitation voltage 30 kV. The samples were coated with 3 nm of gold with a vacuum sputter coater.

The thermogravimetric analysis (TGA) of the treated and untreated BSF/LDPE composites was conducted with a thermogravimetric analyzer (model TG 50) supplied by TA Instruments (New Castle, USA). A 20-mg sample of each type of fiber was taken for analysis. The samples were heated steadily at a rate of 20 K/min from 298 to 773 K under a nitrogen atmosphere. To ensure accuracy, the analysis was done two times for each sample.

RESULTS AND DISCUSSION

Effect of the Fiber Loading

Table II shows the effect of the fiber loading on the density of the BSF/MAPP/LDPE composites. With increasing fiber content, the density of the composites decreased. The UTS, YM, flexural strength (FS), and impact strength (IS) values of the untreated, bleached, and treated BSF/MAPP/LDPE blended composites with respect to different fiber loadings are illustrated in Figures 1–4 to determine the optimum fiber loading needed to achieve the maximum mechanical properties. It is shown in

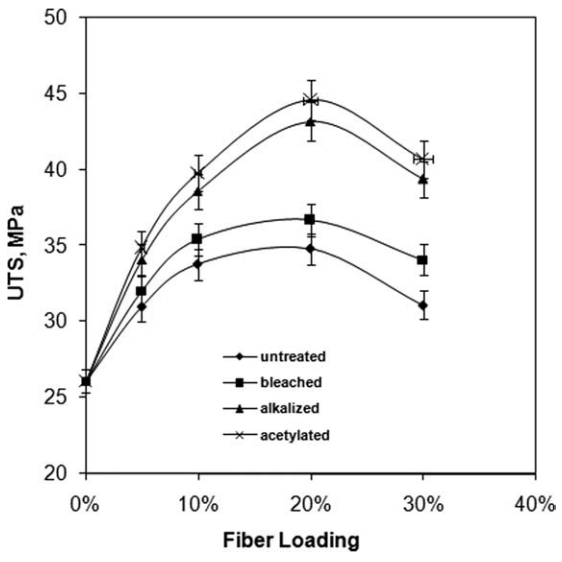

Figure 1. UTS of the untreated and treated BSF/MAPP/LDPE blended composites with fiber loading.

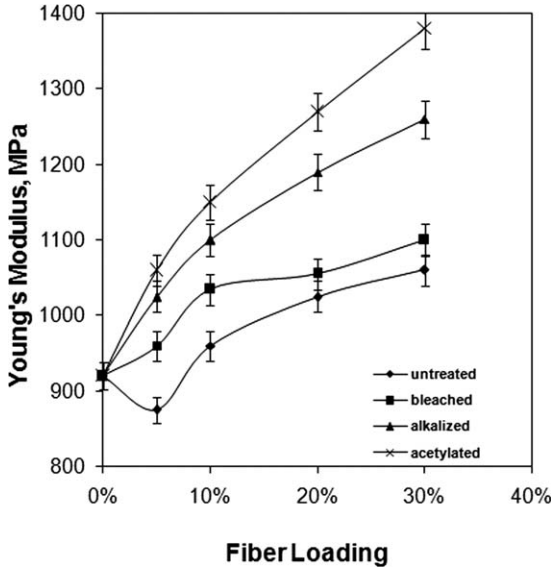

Figure 2. YM of the untreated and treated BSF/MAPP/LDPE blended composites with fiber loading.

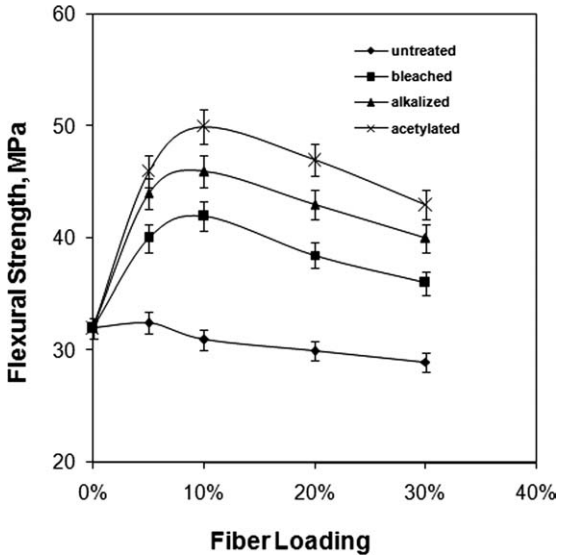

Figure 3. FS of the untreated and treated BSF/MAPP/LDPE blended composites with fiber loading.

Figure 1 that the UTS of the composites increased continuously with increasing fiber loading up to 20%; thereafter, UTS decreased. A smaller quantity of fiber was finely distributed in the matrix, and the interfacial bonding between the fiber and matrix was stronger. Conversely, YM increased with increasing fiber loading, as shown in Figure 2. This may have been due to the fact that crystallites have a much higher modulus compared to amorphous regions and can increase the modulus contribution of the composite.

Figure 3 shows the FS versus fiber loading curves of the LDPE/MAPP/BSF blended composites. FS decreased with increasing fiber loading. The higher FS observed at 10% fiber loading could be explained by a better fiber distribution in the matrix material and fewer fiber fractures. Therefore, the bond between the fiber and the matrix often dictated whether the fiber improved the properties of the composites by transferring an applied load. At a higher fiber loading, the fiber became agglomerated in the composites; hence, FS decreased.

IS is defined as the ability of a material to resist fracture under a stress applied at high speed. The impact properties of composite materials are directly related to their overall toughness. Composite fracture toughness is affected by interlaminar and interfacial strength parameters. The ISs of the BSF/MAPP/LDPE blended composites with different fiber loadings are illustrated in Figure 4. IS was found to increase with an increase in the fiber loading up to 10%; thereafter, IS decreased. This indicated that a lesser amount of fiber had a positive effect on the BSF/MAPP/LDPE blended composites.[26] Similar observations were made by Mohanty et al.[11] Zhang et al.[28] in their research indicated that the total number of defects was predominant at higher fiber loadings. So, the higher fiber loading composites were not well bonded by the matrix, and thus, poor adhesion was obtained.

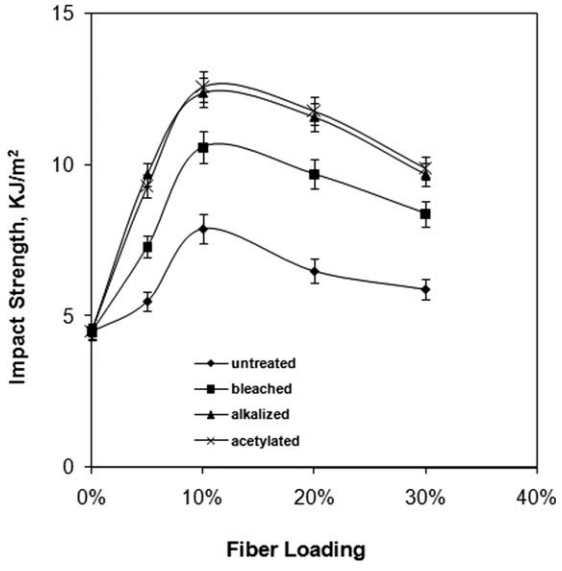

Figure 4. IS of the untreated and treated BSF/MAPP/LDPE blended composites with fiber loading.

Effect of Bleaching

The IR spectra of the bleached fiber [Figure 5(b)] showed changes in the fiber composition during the bleaching treatment. The disappearance of the aromatic C=C bond of lignin around 1500 cm^{-1} proved that lignin was removed completely in the bleaching operation.[25] Also, fibrillation took place in a part of the fiber because of removal of the cementing material (lignin) and hemicellulose; this is shown in Figure 6(b).

The effects of the bleaching of the banana fibers on the TS, YM, FS, and IS values of the BSF/LDPE composites are shown in Figures 1–4, respectively. The bleached BSF/LDPE composites showed a slight enhancement in TS and YM in comparison to the untreated fiber composites. This may have been because of the fibrillation of the fiber, increased surface area, and surface roughness, which gave better interlocking with the LDPE matrix. Again, the crystallinity of the fiber increased with removal of the noncrystalline lignin.[29] Therefore, YM of the bleached BSF/LDPE composites was higher than that of the untreated fiber composites. Similar results were also reported in the

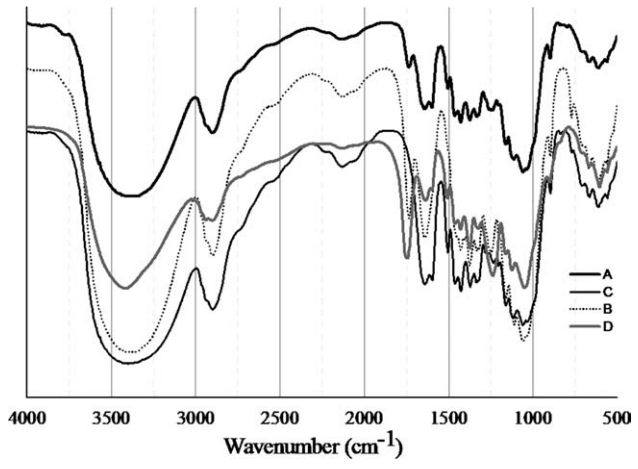

Figure 5. IR spectra of the (A) untreated, (B) bleached, (C) alkali-treated, and (D) acetylated BSF.

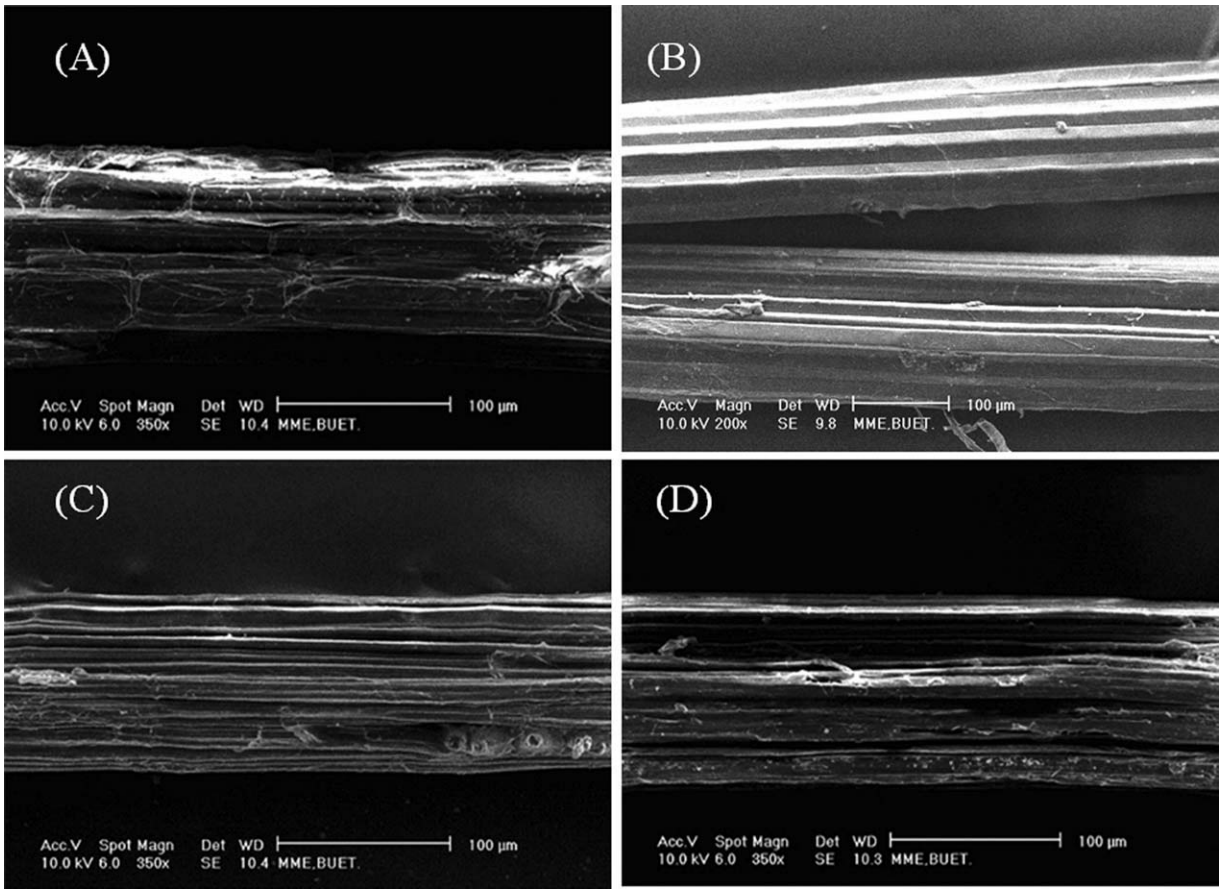

Figure 6. SEM micrographs of the (A) untreated, (B) bleached, (C) alkali-treated, and (D) acetylated BSF.

literature for bleached banana fiber/PP composites.[30] The improved FS may have been due to a lower stiffness and more flexible character of the fibers after delignification. The effect of the bleaching of BSF on the IS values of the resulting composites is shown in Figure 4. The improvement in IS may have been due to better wetting of the bleached fibers with LDPE.

Effect of the Alkali Treatment

Alkali treatment increases the surface roughness and results in better mechanical interlocking and more cellulose exposed on the fiber surface. Several studies have reported that alkalization leads to an increase in amorphous cellulose with the expense of the crystalline part in cellulose and the removal of hydrogen bonds in the network structure.[31–33] The IR spectra of the untreated and bleached BSFs (Figure 5) showed the absorption band at 1740 cm^{-1} because of the C=O stretching vibrations, which disappeared with NaOH treatment. The carboxyl or carbonyl groups present in the fiber as a trace fatty acid were removed during the acid–base reaction. The main spectral changes were an increase in the 898-cm^{-1} band, which was attributed to the symmetric in-phase ring stretching mode, and a decrease in the 1430-cm^{-1} band, which was attributed to CH_2 bending. Similar results were also found for hemp fiber.[34] Figure 6(a–c) are the SEM micrographs of the surfaces of the untreated, bleached, and alkali-treated BSF, respectively. The alkali-treated fiber had a rough surface topography. The development of a rough surface topography and enhancement in aspect ratio offered better fiber/matrix interface addition and increased the mechanical properties.[35]

The effects of NaOH treatment of BSF on the UTS, YM, FS, and IS values of the composites are shown in Figures 1–4, respectively. Improvements in all types of the mechanical strength were observed for the NaOH-treated BSF composites. Figure 7 demonstrates the fracture surface morphologies of the treated and untreated composites that were subjected to flexural load with a 10% fiber loading. SEM observations indicated that there was a considerable difference in the fiber/matrix interaction between the treated and untreated composites. It could be seen in the untreated system [Figure 7(a)] that the phenomenon of pullout occurred to a greater extent than untreated systems [Figure 7(b–d)]. This was probably due to the existence of voids between the matrix and fibers, which led to weak interfacial interactions. The treated systems showed better adhesion compared to the untreated one.

Effect of Acetylation

The influence of the acetylation of BSF on the mechanical properties of the composites is shown in Figures 1–4. It was observed that the UTS, YM, FS, and IS values of the acetylated BSF/MAPP/LDPE blended composites were higher than those of the untreated, bleached, and NaOH-treated fiber composites. With the incorporation of acetylated BSF, the strength of the composites improved by 15–20%. The improvement in the

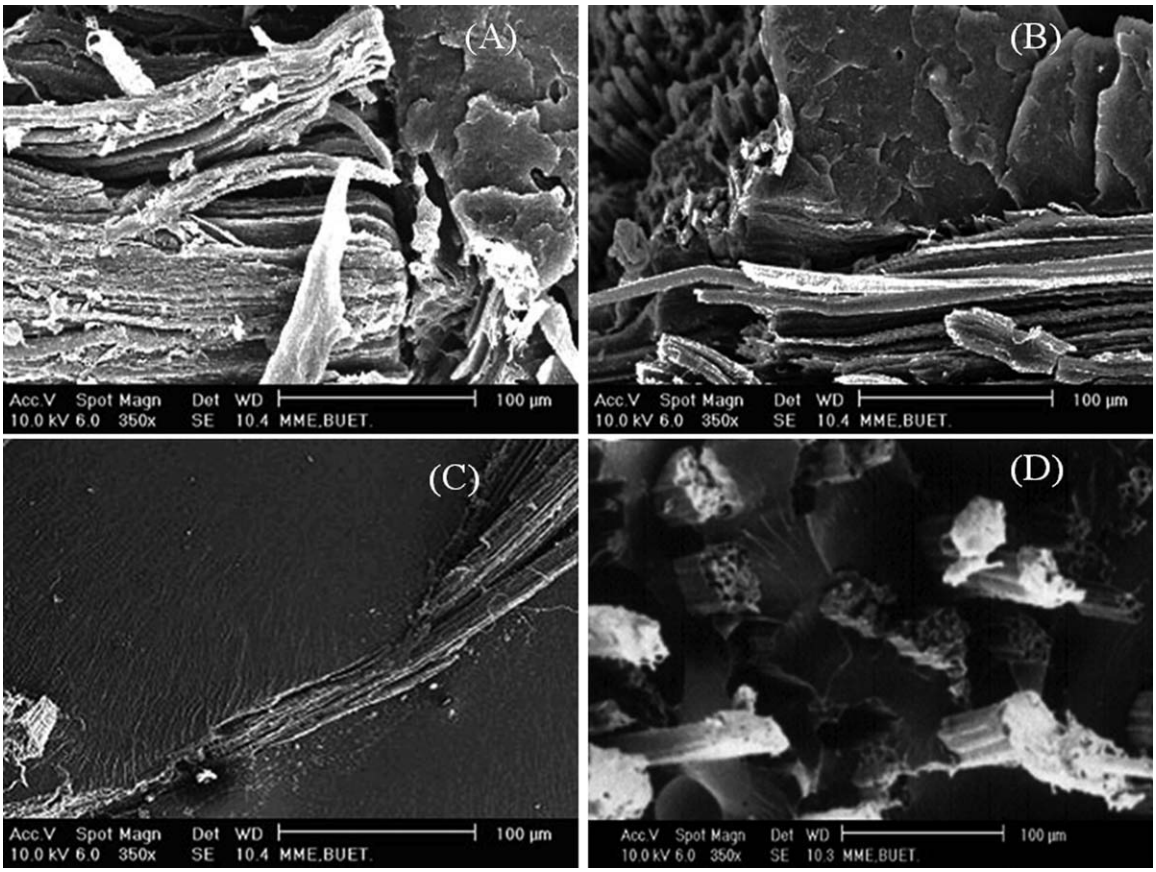

Figure 7. SEM micrographs of the fracture surfaces of the (A) untreated, (B) bleached, (C) alkali-treated, and (D) acetylated BSF (10 wt %)/MAPP/LDPE blended composites.

tensile properties of the acetylated fiber composites was attributed to the presence of —CH_3 groups in the acetylated BSF; this paved the way for its better interaction with the MAPP/LDPE matrix. The —CH_3 groups in the acetylated BSF were less polar than the —OH groups in the untreated, bleached, and alkalized BSF. Thus, the acetylated BSF was more compatible with an inherently nonpolar matrix (LDPE). Moreover, the decrease in the polarity of BSF on acetylation manifested also as a reduction in its hydrophobicity. The change in the chemical structure of the BSF on acetylation was analyzed by IR spectroscopy [Figure 5(d)]. It was seen that the intensity of the —OH peak at 1200–1230 cm^{-1} for the stretching of cellulose was reduced after acetylation as a result of the esterification of the hydroxyl groups. The absorption band formed near 1740 cm^{-1} for acetylated BSF indicated the strong carbonyl stretching frequency corresponding to the carbonyl (C=O) groups present in the ester group.[36] So it was clear that even though there was no direct chemical bond binding acetylated BSF and LDPE, it was the increased hydrophobicity of BSF after treatment that was responsible for the improvement in tensile properties.

The UTS, YM, FS, and IS of the acetylated BSF/LDPE composites were found to be higher than those of the untreated one; this indicated that better interfacial bonding between the matrix and fiber occurred upon chemical treatment. Poor interfacial bonding induced microspaces at the fiber/matrix interface. These microspaces caused microcracks when impact occurred, resulted in crack propagation, and caused a decrease in the IS values of the composites. As a result, the acetylated LDPE/MAPP/BSF composites were capable of absorbing higher amounts of energy to stop crack propagation than the untreated ones.

Table III. Effects of the MAPP Content (w/w %) on the Mechanical Properties of the Acetylated BSF–LDPE Composites

MAPP/LDPE/ acetylated BSF	UTS (MPa)	YM (MPa)	FS (MPa)	IS (kJ/m^2)
0/80/20	38.9 ± 3	1200 ± 2.9	35.1 ± 1.9	8.6 ± 1
1/79/20	40.1 ± 1.2	1210 ± 4.2	36.8 ± 1.9	9.0 ± 1
2/78/20	42.4 ± 2	1250 ± 4.8	38 ± 2.7	9.5 ± 1
5/75/20	47 ± 2	1270 ± 20	44.6 ± 2.4	11.8 ± 1

Table IV. Hybrid Effects of the Untreated and Treated BSF and Coir Fiber MAPP–LDPE Blended Composites

Fiber content (wt %) in the mono and hybrid LDPE composites		UTS (MPa)	YM (MPa)	FS (MPa)	IS (kJ/m^2)
0 wt % BSF	5 wt % coir fiber	26.8 ± 1.3	1310 ± 6.2	21.3 ± 1.5	8.0 ± 0.8
	10 wt % coir fiber	25.9 ± 1.8	1250 ± 5.8	20.7 ± 2.3	8.5 ± 0.8
	15 wt % coir fiber	22.3 ± 2.3	1195 ± 10.3	19.9 ± 2.4	9.0 ± 0.7
10 wt % untreated BSF	0 wt % coir fiber	34.4 ± 2.1	972 ± 4.3	33.4 ± 1.6	7.5 ± 0.9
	5 wt % coir fiber	38.7 ± 2.9	1131 ± 8.6	35.8 ± 2.4	8.2 ± 1.0
	10 wt % coir fiber	36.2 ± 2.6	1089 ± 9.6	32.6 ± 3.4	9.3 ± 1.1
	15 wt % coir fiber	34.5 ± 2.6	1025 ± 10.2	29.5 ± 1.4	9.6 ± 0.8
10 wt % bleached BSF	0 wt % coir fiber	35.5 ± 1.4	1023 ± 2.6	42.1 ± 2.1	10.5 ± 0.7
	5 wt % coir fiber	42.5 ± 2.3	1258 ± 7.6	43.9 ± 2.6	10.6 ± 1.3
	10 wt % coir fiber	40.5 ± 2.4	1165 ± 4.8	42.7 ± 3.1	10.7 ± 1.3
	15 wt % coir fiber	38.1 ± 2.0	985 ± 7.5	39.4 ± 1.9	11.0 ± 1.4
10 wt % alkali treated BSF	0 wt % coir fiber	38.0 ± 1.5	1098 ± 6.2	46.3 ± 1.8	12.0 ± 1.5
	5 wt % coir fiber	49.2 ± 0.9	1420 ± 3.9	48.0 ± 2.1	12.2 ± 1.9
	10 wt % coir fiber	46.8 ± 2.6	1273 ± 12.3	46.1 ± 1.7	12.4 ± 2.1
	15 wt % coir fiber	44.3 ± 3.0	1124 ± 8.8	43.7 ± 2.3	12.5 ± 0.8
10 wt % acetylated BSF	0 wt % coir fiber	40.1 ± 1.9	1160 ± 4.4	50.0 ± 2.1	12.5 ± 0.95
	5 wt % coir fiber	50.0 ± 1.8	1479 ± 3.5	52.4 ± 3.0	12.8 ± 1.0
	10 wt % coir fiber	48.7 ± 1.0	1380 ± 6.4	51.3 ± 1.0	12.9 ± 2.4
	15 wt % coir fiber	46.3 ± 2.8	1207 ± 7.2	48.4 ± 2.7	13.6 ± 2.1

The acetylated BSF was used to observe the effect of the MAPP content in the MAPP/LDPE/BSF blended composites (Table III). Four types of specimens were prepared with ratios of MAPP/LDPE/acetylated BSF of 0 : 80:20, 1 : 79:20, 2 : 78:20, and 5 : 75:20. All of the mechanical properties (UTS, YM, FS, and IS) increased with increasing MAPP content. A similar observation was made for highly crystalline cellulose/PP composites.[37]

Effects of the Hybrid Filler

The reinforcement of two or more fibers in a single matrix leads to hybrid composites with a great diversity of material properties. It appears that the behavior of hybrid composites is simply a weighted sum of the individual components so that there is more favorable balance of properties in the resulting composite material. In this study, hybrid composites were prepared with untreated, bleached, alkali-treated, and acetylated BSF (0 and 10 wt %) in combination with untreated coir fiber (5, 10, and 15 wt %) in an MAPP/LDPE matrix. The effects of the BSF/coir fiber ratio and different types of surface modification, that is, bleaching, alkali treatment, and acetylation, on the UTS, YM, FS, and IS values of the hybrid composites are shown in Table IV.

At all fiber loadings, the tensile strength of the coir fiber/LDPE composite was lower compared to the BSF/LDPE composite and hybrid composites. The composites with 10 wt % BSF and 5 wt % coir fiber showed higher UTS values than those with all other fiber loadings. The UTS of BSF was higher than that of coir fiber (Table IV); this meant that the reinforcing effect of BSF was greater in LDPE than in the coir fiber. The diameter of BSF (180 μm) was less than that of the coir fiber (30 μm) as well. Therefore, the surface area of the fiber in unit area of the composite was higher in the BSF/LDPE composite than in the coir/LDPE composite; this meant that physical interaction and stress transfer in unit area was higher in the case of the BSF-filled composites. As the weight percentage of coir fiber was increased, UTS of the composite decreased. The YMs of the composites are also given in Table IV. The hybrid composites showed a synergism in tensile modulus. The dispersion of fibers was higher in the hybrid composite compared to that of the unhybridized composite.[38] It was reported earlier that the criterion for optimum adhesion between the matrix and its reinforcing fibers is based on maximization of the wetting tension.[39] It was shown that the maximum wetting tension criterion best fulfills two important requirements for a strong interface. First, the physical interactions at the molecular level between the resin and the fibers must be maximized, and second, the liquid resin must spontaneously wet the fiber surface to minimize the flow density at the interface. As the dispersion increases, the wetting tension and physical adhesion between the fiber and matrix increases.

Table IV also delineates the effect of the weight ratio of BSF and coir fiber on FS in the hybrid composites at different fiber loadings. FS of the hybrid composites was higher than that of the unhybridized composites at each fiber loading. FS reached its maximum when the BSF/coir fiber ratio in the composite was 2 : 1. As mentioned earlier, a higher compatibility and dispersion in the hybrid composites was achieved; this led to a better stress-transfer ability in the composites. It was found that when the percentage of coir fiber was increased in the BSF/coir hybrid fiber reinforced LDPE composite, IS increased. A relatively lower compatibility of the fiber increased IS because of the lowest possibility for fiber pullout in the hybrid composites.[23]

Applied Polymer SCIENCE

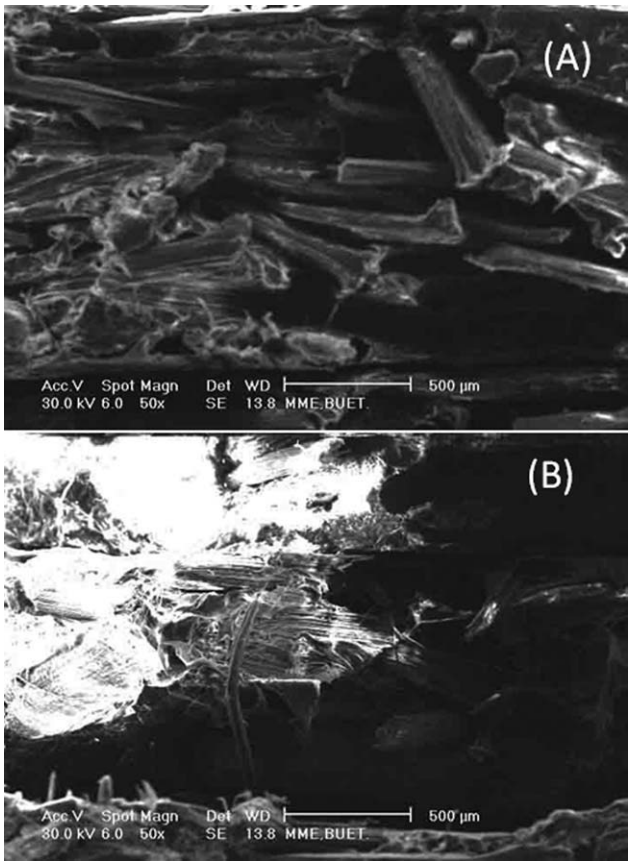

Figure 8. SEM micrographs of the fracture surfaces of (A) BSF (0 wt %)/coir fiber (10 wt %) and (B) BSF (10 wt %)/coir fiber (10 wt %)/MAPP/LDPE blended composites.

The acetylated BSF/coir hybrid LDPE composites showed higher mechanical properties (UTS, YM, FS, and IS) than any other treated, untreated, or hybrid fibers composite. It was mentioned earlier that the acetylated fiber had better compatibility toward the MAPP/LDPE matrix than the other fibers. The other treated BSF/coir hybrid composites also showed better mechanical properties than the untreated BSF/coir hybrid composite. So, in this case, the treated fiber was also dominant in the hybrid filler composites.

It was also revealed that the UTS and tensile modulus of the 10 wt % BSF/10 wt % coir fiber composites was higher than those of the 20 wt % BSF composites. Because of the low density of coir fiber, its composite contained instance gaps between the fiber and the matrix [Figure 8(A)]. On the other hand, high-density BSF sometimes formed clusters in the composites; this decreased the strength and modulus. Also, certain proportions of high-density BSF and low-density coir fiber were well distributed in the composites, as shown in Figure 8(B). Hence, better mechanical properties were found for the hybrid composites.

Effect of the Fiber Constituents

The constituents of BSF were determined by a TAPPI standard method.[27] After aqueous extract, wax, pectin, lignin, or hemicellulose are removed from BSF, it is called deaqueoused fiber, dewaxed fiber, depectinized fiber, delignified fiber, or α-cellulose, respectively. The fibers (10 wt %) were reinforced with LDPE in the presence 5 wt % MAPP and maintained under the previous conditions. The amount of lignin, hemicelluloses, and cellulose in the different fibers and the mechanical properties of their composites were measured; these values are listed in Table V. As shown in the table, the UTS, YM, FS, and IS values of the deaqueoused fiber, dewaxed fiber, depectinized fiber, delignified fiber, and α-cellulose were greater than those of the untreated BSF. The order of UTS, YM, FS, and IS values among the BSF in LDPE composites was Deaqueoused fiber < Dewaxed fiber < Depectinized fiber < Delignified fiber < α-Cellulose. After the noncellulosic matters were removed, the crystallinity and surface roughness of the cellulosic fiber increased through different stages of the chemical treatments.[40] Therefore, good compatibility was found between α-cellulose and MAPP/LDPE.

TGA, Differential Thermogravimetry (DTG), and Differential Thermal Analysis (DTA)

The thermogravimetry (TG) and DTG curves of the untreated, bleached, alkali-treated, and acetylated BSF composites are shown in Figure 9. Here, the initial peak at 303–423 K indicated the removal of moisture from the fiber. The percentage weight loss at this stage was about 2–6%. At 473 K and thereafter, the decomposition of the fiber took place at a faster rate. As shown by the DTG curve, the primary decomposition of the untreated BSF composites occurred at 663 K and corresponded to a weight loss of about 76.3%. This was possibly due to the thermal cleavage of glycoside linkages by transglycosylation, the scission of C—O and C—C bonds, and the loss of α-cellulose from the fiber. A charred residue of carbonaceous products was obtained above 873 K. In the bleached, alkali-treated, and acetylated fibers, the main degradation peak temperature shifted to higher temperatures. An increase of about 15–30 K in the

Table V. Effect of the BSF (10 wt %) Constituents on UTS, YM, FS, and IS of the MAPP–LDPE Composites

LDPE composite	Cellulose (%)	Hemicellulose (%)	Lignin (%)	UTS (MPa)	YM (MPa)	FS (MPa)	IS (kJ/m^2)
Untreated BSF	63–64	19	5	34.4 ± 2.1	972 ± 4.3	33.4 ± 1.6	7.5 ± 0.9
Deaqueoused BSF	66	20	5.5	34.2 ± 1.9	978 ± 5.8	31.5 ± 2.2	8.15 ± 0.8
Dewaxed BSF	66.5	20.2	6.0	35.9 ± 1.0	1062 ± 4.7	32.7 ± 2.6	9.34 ± 0.9
Depectinized BSF	68	21	7.0	36.5 ± 1.6	1085 ± 4.2	33.9 ± 3.3	10 ± 1.0
Delignified BSF	70	23	0.0	40.5 ± 3.1	1163 ± 8.6	37.5 ± 4.0	11.1 ± 1.9
α-Cellulose	95	0.0	0.0	43.7 ± 3.8	1272 ± 9.9	42.3 ± 5.6	11.9 ± 2.3

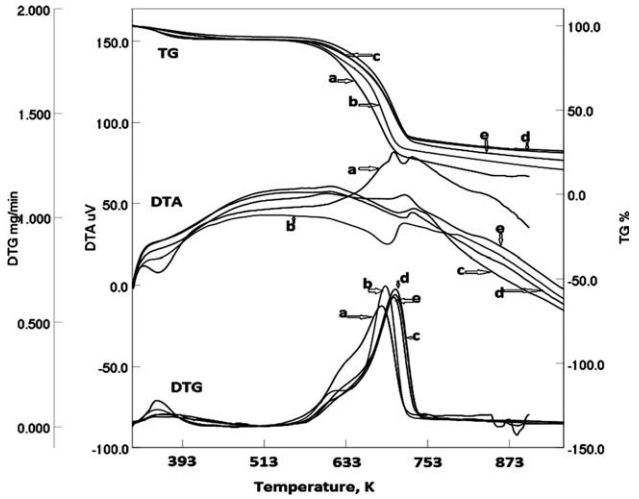

Figure 9. TG, DTA, and DTG curves of the (a) untreated, (b) bleached, (c) alkali-treated, and (d) acetylated BSF (10 wt %)/MAPP/LDPE blended composites and (e) the MAPP/LDPE matrix.

degradation peak and a higher percentage of residue indicated better thermal stability in the treated fibers. This was probably because the treatment reduced hemicellulose in the fiber and, thereby, made the product more thermally stable. Mohanty et al.[41] also reported increased thermal stability in treated sisal fibers. In a comparison of the weight losses at 673 K, weight losses of approximately 76, 70, 52, and 50% were found for the untreated, bleached, alkalized, and acetylated BSF composites. This showed a marginally higher thermal stability in the acetylated composite and, thus, confirmed the presence of intermolecular bonding between the fiber and the matrix due to the formation of ester linkages. The degradation peaks (TG, DTA, and DTG) of the MAPP/LDPE matrix are indicated in Figure 9(e). The degradation temperatures of MAPP/LDPE were almost the same as those of the acetylated and alkalized BSF/MAPP/LDPE composites. This proved that BSF was well bonded with the matrix in the acetylated and alkalized BSF/MAPP/LDPE composites.

The DTA curves of the untreated and treated BSF composites are given in Figure 9. The first endothermic peak was found at 388–393 K due to moisture removal; thereafter, the endothermic peak around 663–693 K indicated the degradation of lignin and cellulose.

CONCLUSIONS

All of the surface treatments improved the mechanical properties of the composites. Among the untreated and treated BSF composites, the acetylated fiber composites showed better mechanical properties. The improvement in the mechanical properties of the acetylated fiber was attributed to the presence of methyl groups, which were more compatible with the nonpolar matrix. The hybrid effects of the BSF/coir fibers on the mechanical properties of the LDPE composites were studied, and the obtained mechanical properties were were superior to those of the unhybridized fiber composites. Interestingly, surface treatment played the major role in determining the mechanical properties of the composites. Therefore, hybrid fiber composites with BSF and coir fiber may open up new applications. The thermal stability of the acetylated and alkalized BSF/MAPP/LDPE composites was much higher than that of the untreated one. Finally, it is worth mentioning that these composites had a woodlike appearance and could be used as a substitute for wood.

ACKNOWLEDGMENTS

The authors gratefully acknowledge the Director, materials and metallurgical engineering (MME) Department, Bangladesh University of Engineering and Technology (BUET), Dhaka, Bangladesh, and Director, Bangladesh Council of Scientific and Industrial Research (BCSIR), Dhaka, Bangladesh, for IR spectroscopy, TGA, SEM, and tensile testing.

REFERENCES

1. Fung, K. L.; Xing, X. S.; Li, R. K. Y.; Tjong, S. C.; Mai, Y. W. *Compos. Sci. Technol.* **2003,** *63*, 1255.
2. Arbelaiz, A.; Fernández, B.; Ramos, J. A.; Retegi, A.; Llano-Ponte, R.; Mondragon, I. *Compos. Sci. Technol.* **2005,** *65*, 1582.
3. Garkhail, S. K.; Heijenrath, R. W. H.; Peijs, T. *Appl. Compos. Mater.* **2000,** *7*, 351.
4. Botev, M.; Betchev, H.; Bikaris, D.; Panayiotou, C. *J. Appl. Polym. Sci.* **1999,** *74*, 523.
5. Bledzki, A. K.; Gassan, J. *Prog. Polym. Sci.* **1999,** *24*, 221.
6. Bos, H. L.; Van den Oever, M. J. A.; Peters, O. C. J. *J. Mater. Sci.* **2002,** *37*, 1683.
7. Mohanty, A. K.; Misra, M.; Hinrichsen, G. *Macromol. Mater. Eng.* **2000,** *276/277*, 1.
8. Gassan, J.; Gutowski, V. S. *Compos. Sci. Technol.* **2000,** *60*, 2857.
9. Mwaikambo, L. Y.; Bisanda, E. T. N. *Polym. Test.* **1999,** *18*, 181.
10. Dikobe, D. G.; Luyt, A. S. *Express Polym. Letters* **2010,** *4*, 729.
11. Rout, J.; Misra, M.; Tripathy, S. S.; Nayak, S. K.; Mohanty, A. K. *Compos. Sci. Technol.* **2001,** *61*, 1303.
12. Belgacem, M. N.; Gandini, A. *Compos. Interfaces* **2005,** *12*, 41.
13. Pasquini, D.; Belgacem, M. N.; Gandini, A.; Curvelo, A. A. D. *J. Colloid. Interface. Sci.* **2006,** *295*, 79.
14. Mehta, G.; Drzal, L. T.; Mohanty, A. K.; Misra, M. *J. Appl. Polym. Sci.* **2006,** *99*, 1055.
15. John, M. J.; Anandjiwala, R. D. *Polym. Compos.* **2008,** *29*, 187.
16. Agrawal, R.; Saxena, N. S.; Sharma, K. B.; Thomas, S.; Sreekala, M. S. *Mater. Sci. Eng. A.* **2000,** *277*, 77.
17. Fisher, T.; Hajaligol, M.; Waymack, B.; Kellogg, D. *J. Anal. Appl. Pyrolysis.* **2002,** *62*, 331.
18. Lee, S. M. International Encyclopaedia of Composites; VHC: New York, **1991;** Vol. 4.
19. Mondal, I. H.; Arifuzzaman Khan, G. M. *Cellulose Chem. Technol.* **2008,** *42*, 9.
20. Jacob, M.; Thomas, S.; Varughese, K. T. *J. Appl. Polym. Sci.* **2004,** *93*, 2305.
21. Jacob, M.; Thomas, S.; Varughese, K. T. *Compos. Sci. Tech.* **2004,** *64*, 955.

22. Paiva Junior, C. Z.; de Carvalho, L. H.; Fonesca, V. M.; Monteiro, S. N.; d'Almeida, J. R. M. *Polym. Test* **2004,** *23*, 131.
23. Idicula, M.; Joseph, K.; Thomas, S. *J. Reinforced Plastics Compos.* **2010,** *29*, 12.
24. Venkateshwaran, N.; Elayaperumal, A. *J. Reinforced Plastics Compos.* **2010,** *29*, 2387.
25. Piedad, G.; Javier, C.; Saioa, G.; Aitor, A.; Iñaki, M. *J. Appl. Polym. Sci.* **2004,** *94*, 1489.
26. Rahman, M. R.; Huque, M. M.; Islam, M. N.; Hasan, M. *Compos. A.* **2009,** *40*, 511.
27. TAPPI Standard Method 360; TAPPI: New York, **1993.**
28. Zhang, M. Q.; Rong, M. Z.; Lu, X. *Compos. Sci. Technol.* **2005,** *65*, 2514.
29. Márcia, A. S. S.; Carlos, S. L.; Karen, K. G. F.; Marco, A. D. P. *Carbohydr. Polym.* **2009,** *77*, 47.
30. Chen, X.; Guo, Q.; Mi Y. *J. Appl. Polym. Sci.* **1998,** *69*, 1891.
31. Mohanty, A. K.; Misra, M.; Drzal, L. T. *Compos. Interfaces* **2000,** *8*, 313.
32. Sreekala, M. S.; Kumaran, M. G.; Joseph, S.; Jacob, M.; Thomas, S. *Appl. Compos. Mater.* **2000,** *7*, 295.
33. Mwaikambo, L. Y.; Ansell, M. P. *J. Appl. Polym. Sci.* **2002,** *84*, 2222.
34. Oujai, S.; Hodzid, A.; Shanks R. A. *J. Appl. Polym. Sci.* **2004,** *94*, 2456.
35. Aziz, S. H.; Ansell M. P. *Compos. Sci. Technol.* **2004,** *64*, 1219.
36. Kalaprasad, G.; Francis, B.; Thomas, S.; Kumar, C. R.; Pavithran, C.; Groeninckx, G.; Thomas, S. *Polym. Int.* **2004,** *53*, 1624.
37. Qiu, W.; Zhabg, F.; Endo, T.; Hirotsu, T. *J. Appl. Sci. Technol.* **2002,** *87*, 337.
38. Kretsis, G. *Composites* **1987,** *18*, 13.
39. Connor, M.; Bidaux, J. E.; Manson, J. A. E. *J. Mater. Sci.* **1997,** *32*, 5059.
40. Alam, M. S.; Khan, G. M. A.; Razzaque, S. M. A. *J. Appl. Sci. Technol.* **2006,** *4*, 87.
41. Mohanty, S.; Verma, S. K.; Nayak, S. K.; Tripathy, S. S. *J. Appl. Polym. Sci.* **2004,** *94*, 1336.